

On the Robustness of Bayesian Neural Networks to Adversarial Attacks

Luca Bortolussi

LUCA.BORTOLUSSI@GMAIL.COM

Department of Mathematics and Geosciences,

University of Trieste, Trieste, Italy;

Modeling and Simulation Group, Saarland University, Saarland, Germany

Ginevra Carbone

GINEVRA.CARBONE@PHD.UNITS.IT

Department of Mathematics and Geosciences,

University of Trieste, Trieste, Italy

Luca Laurenti

L.LAURENTI@TUDELFT.NL

Delft Center of Systems and Control,

TU Delft University, The Netherlands

Andrea Patane

APATANE@TCD.IE

School of Computer Science and Statistics,

Trinity College, Dublin, Ireland

Guido Sanguinetti

GSANGUIN@SISSA.IT

School of Informatics,

University of Edinburgh, Edinburgh, United Kingdom;

SISSA, International School of Advanced Studies, Trieste, Italy.

Matthew Wicker

MATTHEW.WICKER@WOLFSON.OX.AC.UK

Department of Computer Science,

University of Oxford, Oxford, United Kingdom

Abstract

Vulnerability to adversarial attacks is one of the principal hurdles to the adoption of deep learning in safety-critical applications. Despite significant efforts, both practical and theoretical, training deep learning models robust to adversarial attacks is still an open problem. In this paper, we analyse the geometry of adversarial attacks in the large-data, overparameterized limit for Bayesian Neural Networks (BNNs). We show that, in the limit, vulnerability to gradient-based attacks arises as a result of degeneracy in the data distribution, i.e., when the data lies on a lower-dimensional submanifold of the ambient space. As a direct consequence, we demonstrate that in this limit BNN posteriors are robust to gradient-based adversarial attacks. Crucially, we prove that the expected gradient of the loss with respect to the BNN posterior distribution is vanishing, even when each neural network sampled from the posterior is vulnerable to gradient-based attacks. Experimental results on the MNIST, Fashion MNIST, and half moons datasets, representing the finite data regime, with BNNs trained with Hamiltonian Monte Carlo and Variational Inference, support this line of arguments, showing that BNNs can display both high accuracy on clean data and robustness to both gradient-based and gradient-free based adversarial attacks.

Keywords: Bayesian Neural Networks, Adversarial Attacks, Robustness

1. Introduction

Adversarial attacks are small, potentially imperceptible, perturbations of test inputs that can lead to catastrophic misclassifications in high-dimensional classifiers such as deep Neural Networks (NN). Since the seminal work of Szegedy et al. (2013) adversarial attacks have been intensively studied and even highly accurate state-of-the-art deep learning models, trained on very large data sets, have been shown to be susceptible to such attacks (Goodfellow et al., 2014). In the absence of effective defenses, the widespread existence of adversarial examples has raised serious concerns about the security and robustness of models learned from data (Biggio and Roli, 2018). As a consequence, the development of machine learning models that are robust to adversarial perturbations is an essential pre-condition for their application in safety-critical scenarios, such as autonomous driving, where model failures can lead to fatal or costly accidents.

Many adversarial attack strategies are based on identifying directions of high variability in the loss function by evaluating the gradient w.r.t. to the neural network input (Goodfellow et al., 2014; Madry et al., 2017). Since such variability can be intuitively linked to uncertainty in the prediction, Bayesian Neural Networks (BNNs) (Neal, 2012) have been recently suggested as a more robust deep learning paradigm, a claim that has also found empirical support (Feinman et al., 2017; Wicker et al., 2021; Bekasov and Murray, 2018; Liu et al., 2018; Yuan et al., 2020). However, neither the source of this robustness, nor its general applicability are well understood mathematically.

In this paper we show a remarkable property of BNNs: in a suitably defined large data limit, we prove that the gradients of the expected loss function of an infinitely-wide BNN w.r.t. the input vanish. Our analysis shows that adversarial attacks for highly accurate NNs arise from the low dimensional support of the data generating distribution. By averaging over nuisance dimensions, BNNs achieve zero expected gradient of the loss and are thus provably immune to gradient-based adversarial attacks. Specifically, we first show that, for any neural network achieving zero loss, adversarial attacks arise in directions orthogonal to data manifold. Then, we rely on the submanifold extension lemma (Lee, 2013) to show that in the limit of infinitely-wide layers, for any neural network and any weights set there exists another weights set (of the same neural network architecture) achieving the same loss and with opposite loss gradients orthogonal to the data manifold on a given point. Under the assumption of infinitely many data and flat (i.e., uninformative) prior, we then show that by averaging over these weights sets the expectation of the gradient w.r.t. the posterior distribution of a BNN vanishes. Crucially, our results guarantees that, in the limit, BNNs' posteriors are provably robust to gradient-based adversarial attacks even if each neural network sampled from the posterior is vulnerable to such attacks.

We experimentally support our theoretical findings on various BNN architectures trained with Hamiltonian Monte Carlo (HMC) and with Variational Inference (VI) on MNIST, Fashion MNIST and the half-moon data set, empirically showing that the magnitude of the gradients decreases as more samples are taken from the BNN posterior. We then explore the robustness of BNNs to adversarial attacks. In particular, we conduct a large-scale experiment on thousands of different neural networks, empirically finding that, in the cases here analysed, for BNNs high accuracy correlates with high robustness to gradient-based adversarial attacks, contrary to what observed for deterministic NNs trained via standard

Stochastic Gradient Descent (SGD). Finally, we also investigate the robustness of BNNs to gradient-free adversarial attacks, showing that BNNs are substantially more robust than their deterministic counterpart even in this setting.

In summary, this paper makes the following contributions:

- A proof that, in the infinitely-wide layers and large data limit setting, the gradient of the loss function w.r.t. the input only preserves the component which is orthogonal to the data manifold (Section 3) and that for any weights set of a neural network there exists another weight set with same loss and opposite orthogonal gradients (Section 3.1).
- A proof that, in the infinitely wide and large data limit, the posterior average of the gradients of the loss function vanishes, thus providing robustness to BNNs (Section 4).
- Experiments showing empirically that BNNs are more robust to both gradient-based and gradient-free attacks than their deterministic counterpart and can resist the well known accuracy-robustness trade-off (Section 6).¹

A preliminary version of this work appeared in Carbone et al. (2020). This work extends Carbone et al. (2020) in several aspects. In Carbone et al. (2020) we proved that given an infinitely-wide neural network with zero loss and a non-zero orthogonal gradient to the data manifold, there exists another zero-loss neural network with opposite orthogonal gradient and use this result to conjecture that BNNs achieve zero gradients in expectation under a wide enough prior. In this paper, in Theorem 6 this result is proved explicitly. Furthermore, we substantially extended the discussion and improved the empirical analysis with gradient-free adversarial attacks.

The paper is structured as follows. In Section 2 we introduce background on infinitely-wide neural networks and BNNs. In Section 3 we will first show that for highly accurate neural networks the gradient of the loss is non-zero only in directions orthogonal to the data manifold. Then, in Section 3.1 we will prove that for any neural network and weight set there exists another weight set of the same neural network with same loss and opposite orthogonal gradients to the data manifold. By averaging over these weight sets in Section 4 we prove that for a BNN the expected gradient of the loss is zero, thus making them robust to adversarial attacks. Section 5 discusses consequences and limitations of our results. Empirical results in Section 6 will support our theoretical findings.

Related Work The robustness of BNNs to adversarial examples has already been observed empirically in various works (Feinman et al., 2017; Yuan et al., 2020; Michelmore et al., 2020; Pang et al., 2021; Smith and Gal, 2018; Uchendu et al., 2021). However, while these works present empirical evidences on the robustness of BNNs, they do not give any theoretical justification on the mechanisms that lead to BNN robustness. First attempts to understand the robustness properties of BNNs have been considered in Bekasov and Murray (2018); Gal and Smith (2018). In particular, Bekasov and Murray (2018) defined Bayesian adversarial spheres and empirically showed that, for BNNs trained with HMC, adversarial examples tend to have high uncertainty. Gal and Smith (2018) derived sufficient conditions for idealised BNNs to avoid adversarial examples. However, it is unclear how such conditions could be

1. The code for the experiments can be found at <https://github.com/ginevracoal/robustBNNs>.

checked in practice, as it would require one to check that the BNN architecture is invariant under all the symmetries of the data.

Because of the capabilities of BNNs to model uncertainty, which can be intuitively linked to their robustness properties, both empirical (Carlini and Wagner, 2017; Li and Gal, 2017; Feinman et al., 2017; Rawat et al., 2017; Grosse et al., 2018) and formal verification methods (Wicker et al., 2020; Berrada et al., 2021) to detect adversarial examples for BNNs have been introduced. These methods have been followed by techniques to perform adversarial training for BNNs (Zhang et al., 2021; Ye and Zhu, 2018; Liu et al., 2018; Wicker et al., 2021), where additional robustness constraints or penalties are considered directly at training time. Interestingly, empirical results obtained with such techniques, highlighted how, in the Bayesian settings, high accuracy and high robustness often are positively correlated with each other. The theoretical framework we develop in this paper further confirms and grounds these findings.

2. Background

Let $f^{true} : \mathcal{M} \rightarrow \mathbb{R}$ be a function defined on a smooth closed data manifold $\mathcal{M} \subset X \subset \mathbb{R}^d$ with X being the ambient (or embedding) space.² We consider the problem of approximating f^{true} via the learning of an $M + 1$ layers neural network $f(\cdot, \mathbf{w})$, with $\mathbf{w} \in \mathbb{R}^{n_w}$ being the aggregated vector of weights and biases. Formally, for $\mathbf{x} \in X$, $f(\mathbf{x}, \mathbf{w})$ is defined iteratively over the number of layers as:

$$f_i^{(1)}(\mathbf{x}) = \sum_{j=1}^d w_{ij}^{(1)} x_j + b_i^{(1)} \quad (1)$$

$$f_i^{(m)}(\mathbf{x}) = \sum_{j=1}^{n_{m-1}} w_{ij}^{(m)} \phi(f_j^{(m-1)}(\mathbf{x})) + b_i^{(m)}, \quad \text{for } m = 2, \dots, M + 1, \quad (2)$$

$$f(\mathbf{x}, \mathbf{w}) = f^{(M+1)}(\mathbf{x}), \quad (3)$$

where n_m is the number of neurons in the m -th layer, ϕ is the activation function – which we assume to be smooth, bounded, and non-constant. In order to learn the weights of $f(\mathbf{x}, \mathbf{w})$ one considers a dataset D_N composed of N points, $D_N = \{(\mathbf{x}_i, y_i) \mid \mathbf{x}_i \in \mathcal{M}, y_i = f^{true}(\mathbf{x}_i), i = 1, \dots, N\}$. The dataset is hence used to quantify the distance between f^{true} and $f(\cdot, \mathbf{w})$ by evaluating it on a loss function $L(\mathbf{x}, \mathbf{w})$ of the form $L(\mathbf{x}, \mathbf{w}) = \ell(f(\mathbf{x}, \mathbf{w}), f^{true}(\mathbf{x}))$, with $\ell(\cdot, \cdot)$ chosen accordingly to the semantic of the problem at hand (e.g., square loss or cross-entropy).³ Intuitively, minimisation of the loss function over the weight vector \mathbf{w} leads to increasing fit of $f(\mathbf{x}, \mathbf{w})$ to $f^{true}(\mathbf{x})$, with zero-loss indicating that the fit is exact (Bishop et al., 1995), so that the problem of approximating f^{true} boils down to the problem of minimizing the loss function over \mathbf{w} (e.g., by employing gradient descent algorithms).

In this paper, we aim at analysing the adversarial robustness of $f(\mathbf{x}, \mathbf{w})$. In order to do so, we will rely on crucial results from Bayesian learning of neural networks and on the

2. For simplicity of presentation, we assume a scalar output. The results of this paper naturally extend to the multi-output case by treating each output component similarly to the single output case.

3. For simplicity of notation we omit the explicit dependence on the true function from the loss.

properties of infinitely-wide neural networks. The remainder of this section is dedicated to the review of such notions.

2.1 Infinitely-Wide Neural Networks

In our analysis of the behaviour of BNNs under adversarial attacks we rely on the notion of infinitely-wide NNs, i.e. NNs with an infinite number of neurons.

Definition 1 (Infinitely-wide neural network) *Consider a family of neural networks $\{f(\mathbf{x}, \mathbf{w}_{n_w})\}_{n_w > 0}$ of Equations (1)–(3), with a fixed number of neurons for $m = 1, \dots, M - 1$ and a variable number of neurons n_M in the last hidden layer. We say that*

$$f^\infty(\mathbf{x}) := \lim_{n_M \rightarrow \infty} f(\mathbf{x}, \mathbf{w}_{n_w}) \quad \forall \mathbf{x} \in X, \quad (4)$$

is an infinitely wide neural network if the limit above exists and if the resulting function defines a mapping from X to \mathbb{R} . Furthermore, we call \mathcal{F} the set of such limit functions.

The interest behind the set of infinitely-wide neural networks lies in the fact that they are universal approximators (Cybenko, 1989; Hornik, 1991).⁴ More precisely, under the assumption that the true function f^{true} is continuous, we have that:

$$\forall \epsilon > 0, \exists f^* \in \mathcal{F} \text{ s.t. } \forall x \in \mathcal{M}, |f^{true}(x) - f^*(x)| < \epsilon. \quad (5)$$

That is, \mathcal{F} is dense in the space of continuous functions. Furthermore, it is possible to show that any smooth function with bounded derivatives can be represented exactly by an infinitely wide NN with bounded weights norm (i.e. with bounded sum of the squared Euclidean norm of the weights in the network) (Ongie et al., 2020). We will rely on these crucial properties of infinitely-wide neural networks to reason about their behaviour against adversarial attacks. For simplicity, as also common in the literature (Rotskoff and Vanden-Eijnden, 2018), throughout the paper we will assume that the approximation error ϵ in Equation (5) is negligible, that is that there exists an infinitely-wide neural network that can approximate the true function exactly. In formal terms, we will assume that any smooth function $g : X \rightarrow \mathbb{R}$ such that $g|_{\mathcal{M}} = f^{true}$ belongs to \mathcal{F} , where $|_{\mathcal{M}}$ denotes the restriction to the data manifold \mathcal{M} . We remark that the existence of such a neural network does not necessarily mean that it will be automatically found through gradient descent-based training on a finite dataset. However, recent results (Rotskoff and Vanden-Eijnden, 2018) have shown that, under mild conditions, the loss function, as a functional over the distribution over weights of an infinitely wide NN, is a convex functional, and hence the gradient flow of stochastic gradient descent will converge to a unique distribution over weights. That is, given an infinitely wide NN f^∞ and a sequence of datasets $\{D_N\}_{N > 0}$ of cardinality N extracted from the data manifold \mathcal{M} , we have that:

$$\lim_{N \rightarrow \infty} \ell(f_{D_N}^\infty(\mathbf{x}), f^{true}(\mathbf{x})) = 0, \quad \forall \mathbf{x} \in \mathcal{M} \quad (6)$$

4. Notice that the limit in Definition 1 is taken only w.r.t. the last hidden layer. Similar results, albeit with additional care needed for the definition of the limiting sequence, can be obtained by taking the limit w.r.t. all the hidden layers (Matthews et al., 2018).

where $f_{D_N}^\infty$ represents the infinitely wide NN trained on D_N until convergence. In Section 3 we will show how deterministic neural networks can be vulnerable to adversarial attacks even when the loss is zero, while infinitely wide Bayesian neural networks achieving zero loss are provably robust to adversarial attacks.

2.2 Bayesian Neural Networks

Bayesian modelling aims to capture the uncertainty of data driven models by defining ensembles of predictors (Barber, 2012); it does so by turning model parameters into random variables. In the NN scenario, one starts by putting a prior measure over the network weights $p(\mathbf{w})$ (Neal, 2012).⁵ The fit of the network with weights \mathbf{w} to the data D is assessed through the likelihood $p(D|\mathbf{w})$ (Bishop, 2006).⁶ Bayesian inference then combines likelihood and prior via the Bayes theorem to obtain a *posterior* distribution over the NN parameters

$$p(\mathbf{w}|D) \propto p(D|\mathbf{w})p(\mathbf{w}). \quad (7)$$

Unfortunately it is in general infeasible to compute the posterior distribution exactly for non-linear/non-conjugate models such as deep NNs, so that approximate Bayesian inference methods are employed in practice. Asymptotically exact samples from the posterior distribution can be obtained via procedures such as Hamiltonian Monte Carlo (HMC) (Neal et al., 2011), while approximate samples can be obtained more cheaply via Variational Inference (VI) (Blundell et al., 2015). Irrespective of the posterior inference method of choice, Bayesian empirical predictions at a new input \mathbf{x} are obtained from an ensemble of n NNs, each with its individual weights drawn from the posterior distribution $p(\mathbf{w}|D)$:

$$f(\mathbf{x}|D) = \langle f(\mathbf{x}, \mathbf{w}) \rangle_{p(\mathbf{w}|D)} \simeq \frac{1}{n} \sum_{i=1}^n f(\mathbf{x}, \mathbf{w}_i) \quad \mathbf{w}_i \sim p(\mathbf{w}|D) \quad (8)$$

where $\langle \cdot \rangle_{p(\mathbf{w}|D)}$ denotes expectation w.r.t. the posterior distribution $p(\mathbf{w}|D)$.

We notice that defining a distribution over the weights $p(\mathbf{w})$ naturally leads to the definition of a distribution over the functions in \mathcal{F} through the applications of the neural network, which we denote by $p(f(\cdot, \mathbf{w}))$. In particular, $p(f(\cdot, \mathbf{w}))$ leads to a probability measure P over \mathcal{F} with a σ -algebra generated by sets of the form $\{f(\cdot, \mathbf{w}) \in \mathcal{F} : f(\mathbf{x}_1, \mathbf{w}) \in G_1, \dots, f(\mathbf{x}_K, \mathbf{w}) \in G_K\}$ where K is an arbitrary integer, $\mathbf{x}_1, \dots, \mathbf{x}_K \in X$, and $G_1, \dots, G_K \subset \mathbb{R}$ are closed intervals (Adler, 2010). Note that according to the above definition of σ -algebra any measurable set of functions $F \subseteq \mathcal{F}$ only depends on the behaviour of $f(\cdot, \mathbf{w})$ on a countable set of input points. Nevertheless, in our setting this is not limiting. In fact, properties involving uncountable set of points can generally (and this is the case for all the properties considered in this paper) be reformulated over a countable set of inputs by relying on the continuity of each function $f(\cdot, \mathbf{w}) \in \mathcal{F}$ (Adler, 2010).

In this paper, we will rely on flat or uninformative priors (Box and Tiao, 2011; Christensen et al., 2010), that is wide priors that resemble a uniform distribution. We introduce the concept of *flat priors* over the space of functions \mathcal{F} .

5. In the remainder of this paper, we employ the common notation of indicating density functions with p and their corresponding probability measures with P .
6. Notice that in the Bayesian setting the likelihood is a transformation of the loss function used in deterministic settings. In the rest of the paper we use both terminologies, and the loss is not to be confused with that used in Bayesian decision theory (Bishop, 2006).

Definition 2 (Flat Prior) Let p be a prior distribution and P the corresponding probability measure. Then, we say that a prior is flat when for any $K > 0$, if we consider any K points $\mathbf{x}_1, \dots, \mathbf{x}_K \in X$, any closed intervals $G_1, \dots, G_K \subset \mathbb{R}$, and any $g_1, \dots, g_K \in \mathbb{R}$ it holds that

$$P(f(\cdot, \mathbf{w}) \in \mathcal{F} : f(\mathbf{x}_1, \mathbf{w}) \in G_1, \dots, f(\mathbf{x}_K, \mathbf{w}) \in G_K) = \\ P(f(\cdot, \mathbf{w}) \in \mathcal{F} : f(\mathbf{x}_1, \mathbf{w}) \in G_1 + g_1, \dots, f(\mathbf{x}_K, \mathbf{w}) \in G_K + g_K)$$

that is, if its finite-dimensional distributions are translation invariant.

According to Definition 2, a flat prior gives a uniform distribution on the outcomes of $f(\cdot, \mathbf{w})$ for any countable set of input points. Furthermore, as P is uniquely defined through its behaviour on a countable number of input points, Definition 2 implies that for any measurable set of functions $F \subset \mathcal{F}$, function $g \in \mathcal{F}$, and set $F_g = \{f \in \mathcal{F} : \exists f' \in F \text{ s.t. } f = f' + g\}$, it holds that $P(f(\cdot, \mathbf{w}) \in F) = P(f(\cdot, \mathbf{w}) \in F_g)$, that is if we translate a set of function by a given function we obtain the same probability. We should stress that, formally, a prior so defined is not a distribution but an *improper prior*, as the scaling factor for a translation invariant measure defined over an infinite support does not exist (Box and Tiao, 2011). In practice one can approximate a flat prior with a Gaussian distribution with variance that tends to infinity.

Notice that while Definition 2 defines a prior over the space of functions induced by a neural network, in practice, often one would often like to define a prior directly over the weights. In this context, we stress that, for an infinitely-wide BNN, a Gaussian prior with large (finite) variance over the weights induces a Gaussian prior with large variance over the space of functions (Matthews et al., 2018). Thus, assuming a prior $p(\mathbf{w})$ with large variance is in practice a good approximation of a flat prior as per Definition 2. In any case, we should also stress that in this paper we will rely on flat priors on a large data setting, where the influence of a flat prior on the posterior is often limited (Christensen et al., 2010). In this context, a flat prior assumption is necessary to guarantee that all possible functions that can represent the neural network can equally influence the posterior.

2.3 Adversarial Attacks for Bayesian Neural Networks

Given an input point $\mathbf{x} \in \mathcal{M}$ and a strength (i.e. maximum perturbation magnitude) $\epsilon > 0$, the worst-case adversarial perturbation can be defined as the point $\tilde{\mathbf{x}}$ in the ϵ -neighbourhood around \mathbf{x} that maximises the loss function L :

$$\tilde{\mathbf{x}} := \arg \max_{\tilde{\mathbf{x}}: \|\tilde{\mathbf{x}} - \mathbf{x}\| \leq \epsilon} \langle L(\tilde{\mathbf{x}}, \mathbf{w}) \rangle_{p(\mathbf{w}|D)}.$$

If the network prediction on $\tilde{\mathbf{x}}$ differs from the original prediction on \mathbf{x} , then we call $\tilde{\mathbf{x}}$ an *adversarial example*. As $f(\mathbf{x}, \mathbf{w})$ is non-convex, computing $\tilde{\mathbf{x}}$ is a non-convex optimisation problem for which several approximate solution methods have been proposed. In this paper we will primarily focus on what arguably is the most commonly employed class among them, i.e., gradient-based attacks, that is attacks that employ the loss function gradient w.r.t. \mathbf{x} to maximise the loss (Biggio and Roli, 2018). One such attacks is the Fast Gradient Sign Method (FGSM) (Goodfellow et al., 2014) which works by approximating $\tilde{\mathbf{x}}$ by taking an

ϵ -step in the direction of the sign of the gradient at \mathbf{x} . In the context of BNNs, where attacks are against the posterior distribution, applying FGSM yields

$$\tilde{\mathbf{x}} = \mathbf{x} + \epsilon \operatorname{sgn} \langle \nabla_{\mathbf{x}} L(\mathbf{x}, \mathbf{w}) \rangle_{p(\mathbf{w}|D)} \simeq \mathbf{x} + \epsilon \operatorname{sgn} \left(\sum_{i=1}^n \nabla_{\mathbf{x}} L(\mathbf{x}, \mathbf{w}_i) \right) \quad (9)$$

where the final expression is a Monte Carlo approximation with samples \mathbf{w}_i drawn from the posterior $p(\mathbf{w}|D)$. Other gradient-based attacks, as for example Projected Gradient Descent method (PGD) (Madry et al., 2017), modify FGSM by taking consecutive gradient iterations or by scaling the attack by the magnitude of the gradient. Crucially, however, they all rely on the gradient vector to guide the attack. In the following sections, we will show that the expected loss gradient in Equation (9) vanishes to zero for an infinitely-wide Bayesian neural network achieving high accuracy.

3. Gradient-Based Adversarial Attacks for Neural Networks

Equation (9) suggests a possible mechanism through which BNNs might acquire robustness against adversarial attacks: averaging under the posterior might lead to cancellations in the expectation of the gradient of the loss. It turns out that this averaging property is intimately related to the geometry of the data manifold \mathcal{M} . As a consequence, in order to study the expectation of the gradient of the loss for BNNs, we first introduce results that link the geometry of \mathcal{M} to adversarial attacks.

We start with a trivial, yet important result: for a NN that achieves zero loss on the whole data manifold \mathcal{M} , the loss gradient is constant (and zero) along the data manifold for any $\mathbf{x}^* \in \mathcal{M}$. Therefore, in order to have adversarial examples the dimension of the data manifold \mathcal{M} must necessarily be smaller than the dimension of the ambient space, that is, $\dim(\mathcal{M}) < \dim(X) = d$, where $\dim(\mathcal{M})$ denotes the dimension of \mathcal{M} .

Lemma 3 *Assume that $\forall \mathbf{x} \in \mathcal{M} L(\mathbf{x}, \mathbf{w}) = 0$, that is $f(\mathbf{x}, \mathbf{w})$ achieves zero loss on \mathcal{M} . Then, if f is vulnerable to gradient-based attacks at $\mathbf{x}^* \in \mathcal{M}$, $\dim(\mathcal{M}) < \dim(X)$ in a neighbourhood of \mathbf{x}^* , i.e. \mathcal{M} is locally homeomorphic to a space of dimension smaller than the ambient space X .*

Proof By assumption $\forall \mathbf{x} \in \mathcal{M}, L(\mathbf{x}, \mathbf{w}) = 0$, which implies that the gradient of the loss is zero along the data manifold. However, if f is vulnerable to gradient based attacks at \mathbf{x}^* then the gradient of the loss at \mathbf{x}^* must be non-zero. Hence, there exists an open neighbourhood \mathcal{B} of \mathbf{x}^* such that $\mathcal{B} \not\subseteq \mathcal{M}$, which implies $\dim(\mathcal{M}) < \dim(X)$ locally around \mathbf{x}^* . ■

Lemma 3 confirms the widely held conjecture that adversarial attacks may originate from degeneracies of the data manifold (Goodfellow et al., 2014; Fawzi et al., 2018). In fact, it has been already empirically noticed (Khouri and Hadfield-Menell, 2018) that adversarial perturbations often arise in directions normal to the data manifold. The suggestion that lower-dimensional data structures might be ubiquitous in NN problems is also corroborated by recent results (Goldt et al., 2019) showing that the characteristic training dynamics of NNs are intimately linked to data lying on a lower-dimensional manifold. Notice that the implication is only one way; it is perfectly possible for the data manifold to be low dimensional and still not vulnerable at many points.

We note that, as discussed in Section 2.1, at convergence of the training algorithm and in the limit of infinitely-many data, infinitely-wide neural networks are guaranteed to achieve zero loss on the data manifold, satisfying the assumption of Lemma 3. As a result, once an infinitely-wide NN is fully trained, for any $\mathbf{x} \in \mathcal{M}$ the gradient of the loss function is orthogonal to the data manifold as it is zero along the data manifold, i.e., $\nabla_{\mathbf{x}}L(\mathbf{x}, \mathbf{w}) = \nabla_{\mathbf{x}}^{\perp}L(\mathbf{x}, \mathbf{w})$, where $\nabla_{\mathbf{x}}^{\perp}$ denotes the gradient projected into the normal subspace of \mathcal{M} at \mathbf{x} . Note that for a given NN, $\nabla_{\mathbf{x}}^{\perp}L(\mathbf{x}, \mathbf{w})$ is in general non-zero even if the network achieves zero loss on \mathcal{M} , thus explaining the existence of adversarial examples even for very accurate classifiers. Crucially, in Section 3.1 we show that for BNNs, when averaged w.r.t. the posterior distribution, the orthogonal gradient vanishes.

3.1 A Symmetry Property of Neural Networks

Before considering the BNN case, in Proposition 5 below we show a symmetry property of neural networks: given a neural network, we can always find an infinitely-wide NN that has the same loss but opposite orthogonal gradient. In order to prove this result, we first introduce Lemma 4, which is a generalization of the submanifold extension lemma and a key result we leverage. It proves that any smooth function defined on a submanifold \mathcal{M} can be extended to the ambient space, in such a way that the choice of the derivatives orthogonal to the submanifold is arbitrary.

Lemma 4 (Anders et al. (2020)) *Let $T_{\mathbf{x}}\mathcal{M}$ be the tangent space of \mathcal{M} at a point $\mathbf{x} \in \mathcal{M}$. Let $V = \sum_{i=\dim(\mathcal{M})+1}^d v^i \partial_i$ be a conservative vector field along \mathcal{M} which assigns a vector in $T_{\mathbf{x}}\mathcal{M}^{\perp}$ for each $\mathbf{x} \in \mathcal{M}$. For any smooth function $f^{true} : \mathcal{M} \rightarrow \mathbb{R}$ there exists a smooth extension $F : X \rightarrow \mathbb{R}$ such that*

$$F|_{\mathcal{M}} = f^{true},$$

where $F|_{\mathcal{M}}$ denotes the restriction of F to the submanifold \mathcal{M} , and such that the derivative of the extension F is

$$\nabla_{\mathbf{x}}F(\mathbf{x}) = (\nabla_1 f^{true}(\mathbf{x}), \dots, \nabla_{\dim(\mathcal{M})} f^{true}(\mathbf{x}), v^{\dim(\mathcal{M})+1}(\mathbf{x}), \dots, v^d(\mathbf{x}))$$

for all $\mathbf{x} \in \mathcal{M}$.

Notice that in Lemma 4, in $\nabla_{\mathbf{x}}F(\mathbf{x})$, we pick the local coordinates at $\mathbf{x} \in \mathcal{M}$, such that the first set of components parametrises the data manifold. We stress that, as \mathcal{M} is smooth, this is without any loss of generality (Lee, 2013). Lemma 4, together with the universal approximation capabilities of NNs (Hornik, 1991), is employed in Proposition 5 to show that for any possible value \mathbf{v} of the orthogonal gradient to the data manifold in a point, there exists at least two (possibly not unique) different weight vectors that achieve zero loss and have orthogonal gradients respectively equal to \mathbf{v} and $-\mathbf{v}$.

Proposition 5 *Consider a NN f with $M + 1$ layers, last hidden layer of size n_M and an input $\mathbf{x} \in \mathcal{M}$. Then, in the limit of $n_M \rightarrow \infty$ (size of last hidden layer going to infinity), for any smooth function $f^{true} : \mathcal{M} \rightarrow \mathbb{R}$ and vector $\mathbf{v} \in \mathbb{R}^{\dim(X) - \dim(\mathcal{M})}$, there exist $\mathbf{w}_1, \mathbf{w}_2$ such that*

$$f(\cdot, \mathbf{w}_1)|_{\mathcal{M}} = f^{true} = f(\cdot, \mathbf{w}_2)|_{\mathcal{M}} \tag{10}$$

$$\nabla_{\mathbf{x}}^{\perp} f(\mathbf{x}, \mathbf{w}_1) = \mathbf{v} = -\nabla_{\mathbf{x}}^{\perp} f(\mathbf{x}, \mathbf{w}_2). \tag{11}$$

Proof From Lemma 4 we know that there exist smooth extensions F^+ and F^- of f^{true} to the embedding space such that $\nabla_{\mathbf{x}}^\perp F^+(\mathbf{x}) = \mathbf{v} = -\nabla_{\mathbf{x}}^\perp F^-(\mathbf{x})$. As a consequence, to conclude the proof it suffices to apply Theorem 3 in (Hornik, 1991) that guarantees that infinitely-wide neural networks are *uniformly 1-dense* on compacts in $\mathcal{C}^1(X)$, under the assumptions of smooth, bounded, and non-constant activation functions. Specifically, for any $F \in \mathcal{C}^1(X)$ and $\epsilon > 0$, for any compact $X' \subseteq X$ there exists a set of weights \mathbf{w} s.t.

$$\max \left\{ \sup_{\mathbf{x} \in X'} \|F(\mathbf{x}) - f(\mathbf{x}, \mathbf{w})\|_\infty, \sup_{\mathbf{x} \in X'} \|\nabla F(\mathbf{x}) - \nabla f(\mathbf{x}, \mathbf{w})\|_\infty \right\} \leq \epsilon.$$

As $F^+, F^- \in \mathcal{C}^1(X)$, this concludes the proof. ■

Note that by the chain rule, the gradient of the loss is proportional to the gradient of the NN. As a consequence, Proposition 5 guarantees that, for infinitely-wide NNs, for any set of weights achieving the minimum loss, then there exists another set of weights with same loss and opposite orthogonal gradient of the loss w.r.t. the input. This suggests that by averaging over these configurations of the weights one can achieve a robust model that has vanishing expected orthogonal gradient. In the next Section, in Theorem 6 we show this is indeed the case. However, we should already emphasize that such a result does not hold by simply averaging the set of weights w.r.t. any distribution. Intuitively, for this result to hold, it is required that each set of weights achieving a given gradient value has the same measure (w.r.t. the posterior) as the set of weights with the same loss and opposite orthogonal gradient value.

4. Adversarial Robustness via Bayesian Averaging

We are now ready to state Theorem 6, where we show that under the assumption of a flat prior, the posterior of an infinitely-wide BNN achieving zero loss has vanishing orthogonal gradients.

Theorem 6 *Let $f(\mathbf{x}, \mathbf{w})$ be an infinitely-wide BNN trained on a data set D_N composed by N data points with true underlying function $f^{true} : \mathcal{M} \rightarrow \mathbb{R}$. Assume that:*

- *The prior is flat.*
- *For $N \rightarrow \infty$ the posterior distribution of the BNN converges weakly to a distribution that achieves zero loss with probability 1, i.e.,*

$$P(f(\cdot, \mathbf{w}) | D_N) \xrightarrow{d} P(f | D_\infty),$$

where $P(f | D_\infty)$ is such that

$$P\left(\sup_{\mathbf{x} \in \mathcal{M}} |f(\mathbf{x}) - f^{true}(\mathbf{x})| = 0 \mid D_\infty\right) = 1. \tag{12}$$

Then, for any $\mathbf{x} \in \mathcal{M}$ it holds that

$$\langle \nabla_{\mathbf{x}}^\perp f(\mathbf{x}, \mathbf{w}) \rangle_{P(f(\cdot, \mathbf{w}) | D_N)} \rightarrow 0. \tag{13}$$

Proof Without any loss of generality assume that $\dim(X) - \dim(\mathcal{M}) = 1$.⁷ Consider the operator

$$\mathcal{G}_{\mathbf{x}} : f \mapsto \nabla_{\mathbf{x}}^{\perp} f(\mathbf{x}),$$

which is linear and bounded under the boundeness assumption on the derivatives of f . By the Portmanteau theorem, $\mathcal{G}_{\mathbf{x}}$ preserves weak convergence, hence

$$\langle \nabla_{\mathbf{x}}^{\perp} f(\mathbf{x}, \mathbf{w}) \rangle_{p(f(\cdot, \mathbf{w})|D_N)} \rightarrow \langle \nabla_{\mathbf{x}}^{\perp} f(\mathbf{x}) \rangle_{p(f|D_{\infty})}. \quad (14)$$

Then, to prove Equation (13) it is enough to show that

$$\langle \nabla_{\mathbf{x}}^{\perp} f(\mathbf{x}) \rangle_{p(f|D_{\infty})} = 0.$$

In order to do that, we proceed as follows. By definition of expectation we have that

$$\begin{aligned} \langle \nabla_{\mathbf{x}}^{\perp} f(\mathbf{x}) \rangle_{p(f|D_{\infty})} &= \int_{\mathbf{v} \in \mathbb{R}} \mathbf{v} p(\nabla_{\mathbf{x}}^{\perp} f(\mathbf{x}) = \mathbf{v} | D_{\infty}) d\mathbf{v} \\ &= \int_{\mathbf{v} \in \mathbb{R}_{>0}} \mathbf{v} p(\nabla_{\mathbf{x}}^{\perp} f(\mathbf{x}) = \mathbf{v} | D_{\infty}) d\mathbf{v} + \int_{\mathbf{v} \in \mathbb{R}_{<0}} \mathbf{v} p(\nabla_{\mathbf{x}}^{\perp} f(\mathbf{x}) = \mathbf{v} | D_{\infty}) d\mathbf{v}. \end{aligned} \quad (15)$$

If we now can show that for any $\mathbf{v} \in \mathbb{R}$ and $\epsilon \in \mathbb{R}_{>0}$, $P(\nabla_{\mathbf{x}}^{\perp} f(\mathbf{x}) \in [\mathbf{v} - \epsilon, \mathbf{v} + \epsilon] | D_{\infty}) := \int_{[\mathbf{v} - \epsilon, \mathbf{v} + \epsilon]} p(\nabla_{\mathbf{x}}^{\perp} f(\mathbf{x}) = v | D_{\infty}) dv$ is constant w.r.t. \mathbf{v} , then this guarantees that Eqn (15) is zero. In fact, by application of the fundamental theorem of calculus, the above implies that for any \mathbf{v} , $p(\nabla_{\mathbf{x}}^{\perp} f(\mathbf{x}) = \mathbf{v} | D_{\infty}) = p(\nabla_{\mathbf{x}}^{\perp} f(\mathbf{x}) = -\mathbf{v} | D_{\infty})$ almost surely (i.e. with probability 1), hence terms in Eqn (15) cancel out. We prove that $P(\nabla_{\mathbf{x}}^{\perp} f(\mathbf{x}) \in [\mathbf{v} - \epsilon, \mathbf{v} + \epsilon] | D_{\infty})$ is constant wrt \mathbf{v} in what follows.

By assumption it holds that any $f \sim P(\cdot | D_{\infty})$ is such that $\forall \bar{\mathbf{x}} \in \mathcal{M}, f(\bar{\mathbf{x}}) = f^{true}(\bar{\mathbf{x}})$ almost surely. Hence, to conclude, being our prior invariant to translations (see Definition 2), it is enough to show that for any \mathbf{v}, \mathbf{v}' sets

$$F_{\mathbf{v}} = \{g \in \mathcal{F} : \forall \bar{\mathbf{x}} \in \mathcal{M}, g(\bar{\mathbf{x}}) = f^{true}(\bar{\mathbf{x}}) \wedge \nabla_{\mathbf{x}}^{\perp} g(\mathbf{x}) \in [\mathbf{v} - \epsilon, \mathbf{v} + \epsilon]\}$$

$$F_{\mathbf{v}'} = \{g \in \mathcal{F} : \forall \bar{\mathbf{x}} \in \mathcal{M}, g(\bar{\mathbf{x}}) = f^{true}(\bar{\mathbf{x}}) \wedge \nabla_{\mathbf{x}}^{\perp} g(\mathbf{x}) \in [\mathbf{v}' - \epsilon, \mathbf{v}' + \epsilon]\}$$

are equal up to a translation. This can be shown as follows. Using Lemma 4 we extend f^{true} to a smooth function $f_{\mathbf{v}}$ in X such that its orthogonal gradient in $\mathbf{x} \in \mathcal{M}$ equals \mathbf{v} , i.e. $\nabla_{\mathbf{x}}^{\perp} f_{\mathbf{v}}(\mathbf{x}) = \mathbf{v}$. Then, because of the linearity of the gradient operator, any other function g on X that is equal to f^{true} when restricted to \mathcal{M} and such that $\nabla_{\mathbf{x}}^{\perp} g(\mathbf{x}) \in [\mathbf{v} - \epsilon, \mathbf{v} + \epsilon]$ can be written as

$$g(\mathbf{x}) = f_{\mathbf{v}}(\mathbf{x}) + \bar{k}(\mathbf{x}),$$

where \bar{k} is a function that has the orthogonal gradient in \mathbf{x} within $[-\epsilon, \epsilon]$ and that is 0 on \mathcal{M} , i.e.,

$$k \in \mathcal{K} = \{\bar{k} : \forall \bar{\mathbf{x}} \in \mathcal{M}, \bar{k}(\bar{\mathbf{x}}) = 0 \wedge \nabla_{\mathbf{x}}^{\perp} \bar{k}(\mathbf{x}) \in [-\epsilon, \epsilon]\}. \quad (16)$$

7. In the case that $\dim(X) - \dim(\mathcal{M}) > 1$, because of the linearity of the partial derivatives, any component of $\langle \nabla_{\mathbf{x}}^{\perp} f(\mathbf{x}) \rangle_{p(f|D_{\infty})}$ can be treated analogously to the case $\dim(X) - \dim(\mathcal{M}) = 1$.

Let's consider a function $f_{\mathbf{v}'}$ built similarly as $f_{\mathbf{v}}$, then we obtain that all $g'(\mathbf{x})$ equal to the true function and such that $\nabla_{\mathbf{x}}^{\perp} g'(\mathbf{x}) = [\mathbf{v}' - \epsilon, \mathbf{v}' + \epsilon]$ can be written as

$$g'(\mathbf{x}) = f_{\mathbf{v}'}(\mathbf{x}) + \bar{k}(\mathbf{x}),$$

with $\bar{k} \in \mathcal{K}$, where \mathcal{K} is as in Equation (16). It then follows that the sets $F_{\mathbf{v}}$ and $F_{\mathbf{v}'}$ are such that $F_{\mathbf{v}} = F_{\mathbf{v}'} + (f_{\mathbf{v}} - f_{\mathbf{v}'})$. Hence, $P(\nabla_{\mathbf{x}}^{\perp} f(\mathbf{x}) \in [\mathbf{v} - \epsilon, \mathbf{v} + \epsilon] \mid D_{\infty}) = P(\nabla_{\mathbf{x}}^{\perp} f(\mathbf{x}) \in [\mathbf{v}' - \epsilon, \mathbf{v}' + \epsilon] \mid D_{\infty})$. Thus, concluding the proof. ■

The proof of Theorem 6 relies on two main assumptions: 1) the prior is flat, which guarantees that probabilities are invariant with respect to translations, thus allowing for perfect cancellation in expectation, 2) the limiting distribution of an infinitely-wide BNN has zero loss with probability 1, which allows us to only focus on the set of functions that are equal to the true functions on the data manifold almost surely. While we will discuss the implication of the flat prior assumption in Section 5, we would like to stress in here that because of the universal approximation properties of neural networks, the second assumption in Theorem 6 is a standard assumption to require, as it guarantees that our posterior converges to the true function with infinitely many data. For example, under mild assumptions, a similar requirement has been explicitly shown to hold for infinitely-wide feed-forward Bayesian neural networks with one hidden layer (Lee, 2000).

Remark 7 *A key aspect in the proof of Theorem 6 is that when the data manifold has a dimension smaller than the ambient space, then there are multiple weight sets minimizing the loss (see Lemma 4) and the BNN posterior averages between them achieving vanishing orthogonal gradients. Note that, if there were just one set of minimizing weights, we could have employed standard results of asymptotic statistics, such as the Bernstein von Mises (BVM) Theorem to study the asymptotic behaviour of the BNN (Vaart, 2000). However, a standard application of the BVM Theorem would have led to a convergence to a Gaussian distribution centered in the maximum likelihood parameters and with vanishing variance: this would have implied that a BNN is robust if and only if also the correspondent deterministic NN with fixed (deterministic) weights is robust, which we know not to be the case. We also confirm this empirically in Figure 6 in the Appendix.*

5. Consequences and Limitations of our Results

The results in the previous section, and in particular of Theorem 6, have the natural consequence of protecting BNNs against all gradient-based attacks, due to the vanishing average of the expectation of the gradients in the limit. Its proof also sheds light on a number of observations made in recent years. Before moving on to empirically validating the theorem in the finite-data and finite-width case, it is worth reflecting on some of its implications and limitations:

- Theorem 6 is proven under the assumption of flat priors needed to require perfect gradient cancellation; in practice, unless the priors are too informative with restrictive

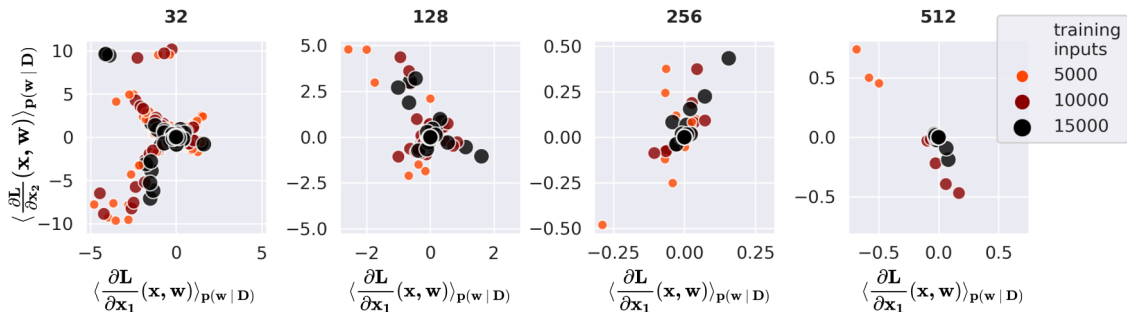


Figure 1: Expected loss gradients components on 100 two-dimensional test points from the Half Moons dataset (Rozza et al., 2014) (both partial derivatives of the loss function are shown). We used a collection of HMC BNNs, by varying the number of hidden neurons (a different number in each subplot) and training points (different color and size of dots). Each dot represents a different NN. Only models with test accuracy greater than 80% were taken into account.

support, we do not expect a major deviation from the idealised case. This is confirmed both from our experimental results and by the fact that in the limit of large data-set the posterior is less influenced by the choice of the prior (Vaart, 2000).

- Theorem 6 holds in a specific thermodynamic limit, however we expect the averaging effect of BNN gradients to still provide considerable protection in conditions where the network architecture and the data amount lead to high accuracy and strong expressivity. In practice, high accuracy might be a good indicator of robustness for BNNs. An empirical confirmation of this result is shown in Figure 1, we examine the impact of the assumptions made in Theorem 6: by exploiting a setting in which we have access to the data-generating distribution, the half-moons dataset (Rozza et al., 2014). We show that the magnitude of the expectation of each component of the gradient shrinks as we increase the number of network’s parameters and the number of training points.
- Theorem 6 holds when the ensemble is drawn from the true posterior; nevertheless cheaper approximate Bayesian inference methods which retain ensemble predictions such as VI may still in practice provide good protection.
- Gaussian Processes (Williams and Rasmussen, 2006) are equivalent to infinitely wide BNNs. Theorem 6 provides theoretical backing to recent empirical observations of their adversarial robustness (Cardelli et al., 2019b; Grosse et al., 2021; Patane et al., 2022).
- While the Bayesian posterior ensemble may not be the only randomization to provide protection, it is clear that some simpler randomizations such as bootstrap will be ineffective, as noted empirically by Bekasov and Murray (2018). This is because bootstrap resampling introduces variability along the data manifold, rather than in orthogonal directions. In this sense, bootstrap clearly cannot be considered a Bayesian approximation, especially when the data distribution has zero measure support w.r.t. the ambient space. Similarly, we do not expect gradient smoothing approaches to be successful (Athalye et al., 2018), since the type of smoothing performed by Bayesian inference is specifically informed by the geometry of the data manifold.

- Theorem 6 only guarantees protection against gradient-based adversarial attacks. As a consequence, it is not clear if the robustness properties of BNNs also extend to non-gradient based attacks. In Section 6.4 we empirically show that the vanishing gradient properties of BNNs also guarantee robustness to non-gradient based attacks.

6. Empirical Results

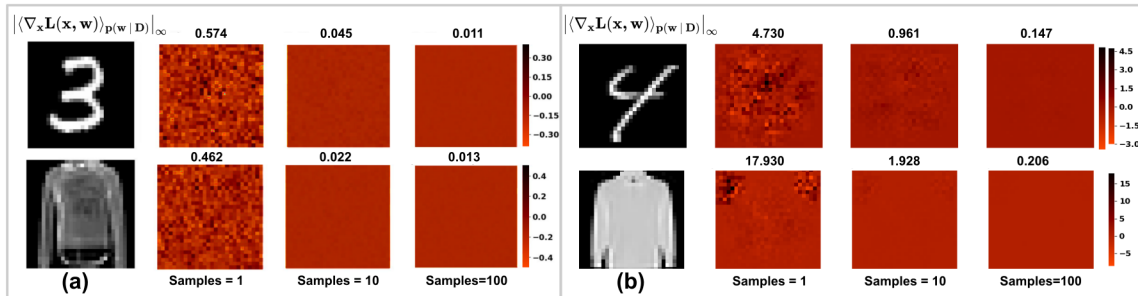


Figure 2: The expected loss gradients of BNNs exhibit a vanishing behaviour when increasing the number of samples from the posterior predictive distribution. We show example images from MNIST (top row) and Fashion MNIST (bottom row) and their expected loss gradients w.r.t. BNNs trained with HMC (left) and VI (right). To the right of the images, we plot a heat map of gradient values.

In this section we empirically investigate our theoretical findings on different BNNs. We train a variety of BNNs on the MNIST and Fashion MNIST (Xiao et al., 2017) datasets, and evaluate their posterior distributions using HMC and VI approximate inference methods. In Section 6.1, we experimentally verify the validity of the zero-averaging property of gradients implied by Theorem 6, and discuss its implications on the behaviours of FGSM and PGD attacks on BNNs in Section 6.2. In Section 6.3 we analyse the relationship between robustness and accuracy on thousands of different NN architectures, comparing the results obtained by Bayesian and by deterministic training. Further, in Section 6.4 we investigate the robustness of BNNs on a gradient-free adversarial attack (Athalye et al., 2018). Details on the experimental settings and BNN training parameters can be found in Appendix B.

6.1 Evaluation of the Gradient of the Loss for BNNs

We investigate the vanishing behavior of input gradients - established by Theorem 6 for the limit regime - in the finite, practical settings, that is with a finite number of training data and with finite-width BNNs. Specifically, for each inference method we perform hyperparameter tuning and select the architecture achieving the highest test accuracy: we train a two hidden layers BNN (with 1024 neurons per layer) with HMC and a three hidden layers BNN (512 neurons per layer) with VI. These achieve approximately 95% test accuracy on MNIST and 89% on Fashion MNIST when trained with HMC; as well as 95% and 92%, respectively, when trained with VI. More details about the hyperparameters used for training can be found in Appendix B.

Figure 2 depicts anecdotal evidence on the behaviour of the component-wise expectation of the loss gradient as more samples from the posterior distribution are incorporated into the BNN predictive distribution. Similarly to how in Figure 1 for the half-moons dataset we observe that the gradient of the loss goes to zero when increasing number of training points and number of parameters, here we have that, as the number of samples taken from the posterior distribution of \mathbf{w} increases, all the components of the gradient approach zero. Notice that the gradient of the individual NNs (that is those with just one sampled weight vector), is far away from being zero. As shown in Theorem 6, it is only through the Bayesian averaging of ensemble predictors that the gradients cancel out.

This is confirmed in Figure 3, where we provide a systematic analysis of the aggregated gradient convergence properties on 1k test images for MNIST and Fashion-MNIST. Each dot shown in the plots represents a component of the expected loss gradient from each one of the images, for a total of 784k points used to visually approximate the empirical distribution of the component-wise expected loss gradient. For both HMC and VI the magnitude of the gradient components drops as the number of samples increases, and tends to stabilize around zero already with 100 samples drawn from the posterior distribution, suggesting that the conditions laid down in Theorem 6 are approximately met by the BNN analysed here. Notice that the gradients computed on HMC trained networks drops more quickly and towards a smaller value compared to VI trained networks. This is in accordance to what is discussed in Section 5, as VI introduces additional approximations in the Bayesian posterior computation.

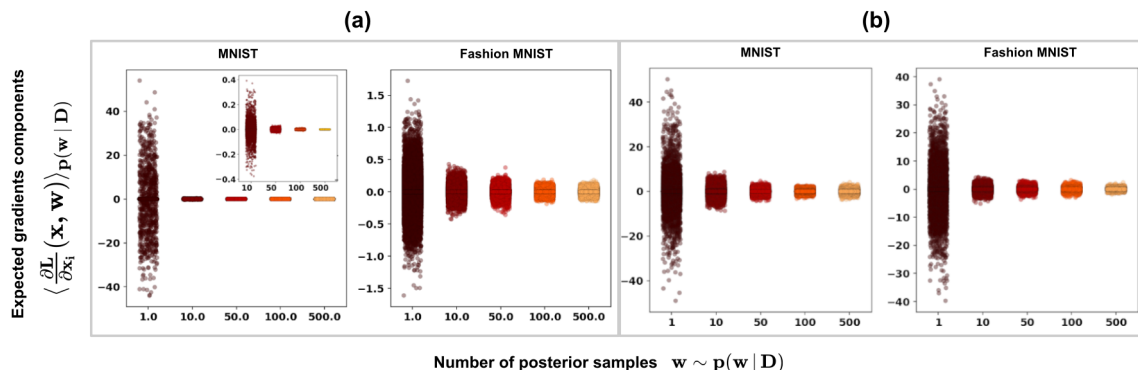


Figure 3: The components of the expected loss gradients approach zero as the number of samples from the posterior distribution increases. For each number of samples, the figure shows 784 gradient components for 1k different test images, from both the MNIST and Fashion MNIST datasets. The gradients are computed on HMC (a) and VI (b) trained BNNs.

6.2 Gradient-Based Attacks for BNNs

The fact that gradient cancellation occurs in the limit does not directly imply that BNNs' predictions are robust to gradient-based attacks in the finite case. For example, FGSM attacks are crafted such that the direction of the manipulation is given only by the sign of the expectation of the loss gradient and not by its magnitude. Thus, even if the entries of the

expectation drop to an infinitesimal magnitude but maintains a meaningful sign, then FGSM could potentially produce effective attacks. In order to test the implications of vanishing gradients on the robustness of the posterior predictive distribution against gradient-based attacks, we compare the behaviour of FGSM and PGD⁸ attacks to a randomly devised attack.

Namely, the random attack mimics a randomised version of FGSM in which the sign of the attack is sampled at random. In practice, we perturb each component of a test image by a random value in $\{-\epsilon, \epsilon\}$. In Table 1 we compare the effectiveness of FGSM, PGD and of the random attack and report the adversarial robustness for 500 images. For each image, we compute the expected gradient using 250 posterior samples. The attacks were performed

Dataset/Method	Rand	FGSM	PGD
MNIST/HMC	0.850	0.960	0.970
MNIST/VI	0.956	0.936	0.938
Fashion/HMC	0.812	0.848	0.826
Fashion/VI	0.744	0.834	0.916

with $\epsilon = 0.1$ and using the categorical cross-entropy loss function. In almost all cases, we see that the random attack outperforms the gradient-based attacks, showing how the vanishing behaviour of the gradient makes FGSM and PGD attacks ineffective. Furthermore, in Table 2 in Appendix A.2 we also run the same evaluation for when the same network employed in Table 1 is trained with SGD and deep ensembles. In both cases both FGSM and PGD are effective, suggesting how simply model averaging and mini-batches are not enough to achieve a robust model.

Table 1: Adversarial robustness of BNNs trained with HMC and VI with respect to the *random attack* (Rand), FGSM and PGD.

6.3 Robustness Accuracy Analysis in Deterministic and Bayesian Neural Networks

In Section 5, we noticed that as a consequence of Theorem 6, high accuracy might be related to high robustness to gradient-based attacks for BNNs. Notice, that this would run counter to what has been observed for deterministic NNs trained with SGD (Su et al., 2018).

In this section, we look at an array of more than 1000 BNNs with different hyperparameters trained with HMC and VI on MNIST and Fashion-MNIST. We experimentally evaluate their accuracy/robustness trade-off on FGSM attacks as compared to that of the same neural network architectures trained via standard (i.e., non-Bayesian) SGD based methods. For the robustness evaluation we consider the average difference in the softmax prediction between the original test points and the crafted adversarial input, as this provides a quantitative and smooth measure of adversarial robustness that is closely related with mis-classification ratios (Cardelli et al., 2019a). That is, for a collection of N test point, we compute

$$\frac{1}{N} \sum_{j=1}^N \left| \langle f(\mathbf{x}_j, \mathbf{w}) \rangle_{p(\mathbf{w}|D)} - \langle f(\tilde{\mathbf{x}}_j, \mathbf{w}) \rangle_{p(\mathbf{w}|D)} \right|_{\infty}. \quad (17)$$

The results of the analysis are plotted in Figure 4 for MNIST and Fashion MNIST. Each dot in the scatter plots represents the results obtained for each specific network architecture

⁸. With 15 iterations and 1 restart.

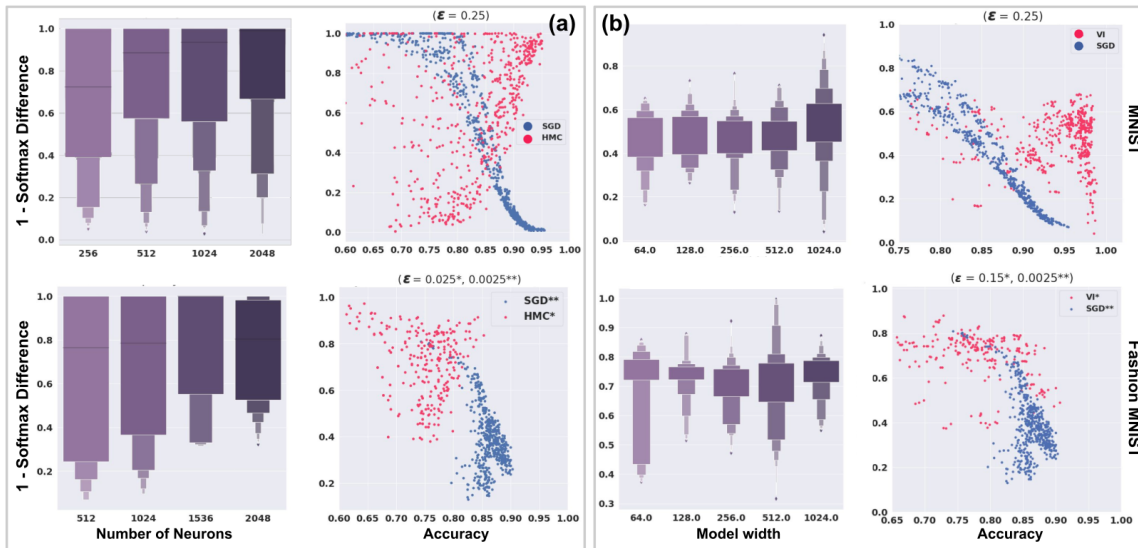


Figure 4: Robustness-Accuracy trade-off on MNIST (first row) and Fashion MNIST (second row) for BNNs trained with HMC (a), VI (b) and SGD (blue dots). While a trade-off between accuracy and robustness occur for deterministic NNs, experiments on HMC show a positive correlation between accuracy and robustness. The boxplots show the correlation between model capacity and robustness. Different attack strength (ϵ) are used for the three methods accordingly to their average robustness.

trained with SGD (blue dots), HMC (pink dots in plots (a)) and VI (pink dots in plots (b)). As already reported in the literature (Su et al., 2018) we observe a marked trade-off between accuracy and robustness (i.e., 1 - softmax difference) for high-performing deterministic networks. Interestingly, this trend is fully reversed for BNNs trained with HMC (plots (a) in Figure 4) where we find that as networks become more accurate, they additionally become more robust to FGSM attacks as well. We further examine this trend in the boxplots that represent the effect that the network width has on the robustness of the resulting posterior. We find the existence of an increasing trend in robustness as the number of neurons in the network is increased. This is in line with our theoretical findings, i.e., as the BNN approaches the infinite width limit, the conditions for Theorem 6 are approximately met and the network is protected against gradient-based attacks.

On the other hand, the trade-off behaviours are less obvious for the BNNs trained with VI and on Fashion-MNIST. In particular, in plot (b) of Figure 4 we find that, similarly to the deterministic case, also for BNNs trained with VI, robustness seems to have a negative correlation with accuracy. Furthermore, for VI we observe that there is some trend dealing with the size of the model, but we only observe this in the case of VI trained on MNIST where it can be seen that model robustness may increase as the width of the layers increases, but this can also lead to poor robustness (which may be indicative of mode collapse).

6.4 Gradient-Free Adversarial Attacks

In this section, we empirically evaluate the most accurate BNN posteriors on MNIST and FashionMNIST from Figure 4 against gradient-free adversarial attacks. Specifically, we consider ZOO (Chen et al., 2017), a gradient-free adversarial attack based on a finite-difference approximation of the gradient of the loss obtained by querying the neural network (in the BNN case the attacker queries the posterior distribution). In particular, we selected ZOO because it has been shown to be effective even when tested on networks that purposefully obfuscate their gradients or have vanishing gradients (Athalye et al., 2018). In Figure 5 we observe that similarly to gradient-based methods, ZOO is substantially less effective on BNNs compared to deterministic NNs in all cases, with BNNs again achieving both high accuracy and high robustness simultaneously. Furthermore, once again HMC is more robust to the attack than VI, which is in turn substantially more robust than deterministic NNs. This suggests how, similarly to what observed in the previous subsections, a more accurate posterior distribution may lead to a more robust model also to gradient-free adversarial attacks.

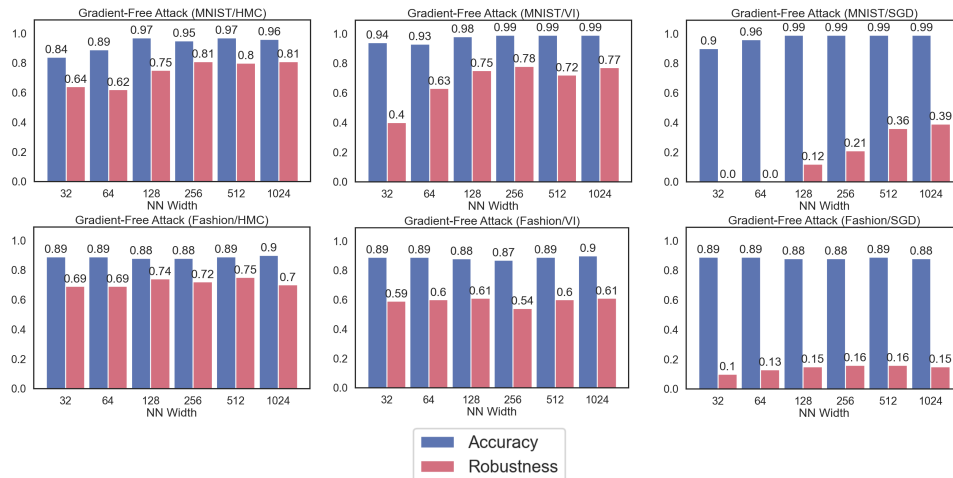


Figure 5: Gradient-free adversarial attacks on BNNs display similar behavior to gradient-based attacks. We evaluate the more accurate networks from Figure 4 with gradient-free attacks on MNIST (first row) and Fashion MNIST (second row) for BNNs trained with HMC (left column), VI (center column), and SGD (right column). We use the same attack parameters as in the Figure 4, but use ZOO as an attack method.

7. Conclusions

The quest for robust, data-driven models is an essential component towards the construction of AI-based technologies. In this respect, we believe that the fact that Bayesian ensembles of NNs can evade a broad class of adversarial attacks will be of great relevance. While promising, this result comes with some significant limitations. First, our theoretical results hold in a thermodynamic limit, which is never realised in practice. More worryingly, we currently have no rigorous diagnostics to understand how near we are to the limit case, and

can only reason about this empirically. Secondly, and perhaps more importantly, performing Bayesian inference in large non-linear models is extremely challenging. In fact, while in our experiments cheaper approximations, such as VI, also enjoyed a degree of adversarial robustness, albeit reduced, there are no guarantees that this will hold in general. To this end, we hope that this result will spark renewed interest in the pursuit of efficient Bayesian inference algorithms.

References

- R. J. Adler. *The geometry of random fields*. SIAM, 2010.
- C. Anders, P. Pasliev, A.-K. Dombrowski, K.-R. Müller, and P. Kessel. Fairwashing explanations with off-manifold detergent. In *International Conference on Machine Learning*, pages 314–323. PMLR, 2020.
- A. Athalye, N. Carlini, and D. Wagner. Obfuscated gradients give a false sense of security: Circumventing defenses to adversarial examples. *arXiv preprint arXiv:1802.00420*, 2018.
- D. Barber. *Bayesian reasoning and machine learning*. Cambridge University Press, 2012.
- A. Bekasov and I. Murray. Bayesian adversarial spheres: Bayesian inference and adversarial examples in a noiseless setting. *arXiv preprint arXiv:1811.12335*, 2018.
- L. Berrada, S. Dathathri, R. Stanforth, R. Bunel, J. Uesato, S. Gowal, M. P. Kumar, et al. Verifying probabilistic specifications with functional lagrangians. *arXiv preprint arXiv:2102.09479*, 2021.
- B. Biggio and F. Roli. Wild patterns: Ten years after the rise of adversarial machine learning. *Pattern Recognition*, 84:317–331, 2018.
- C. M. Bishop. *Pattern Recognition and Machine Learning (Information Science and Statistics)*. Springer-Verlag, Berlin, Heidelberg, 2006. ISBN 0387310738.
- C. M. Bishop et al. *Neural networks for pattern recognition*. Oxford university press, 1995.
- C. Blundell, J. Cornebise, K. Kavukcuoglu, and D. Wierstra. Weight uncertainty in neural networks. *arXiv preprint arXiv:1505.05424*, 2015.
- G. E. Box and G. C. Tiao. *Bayesian inference in statistical analysis*. John Wiley & Sons, 2011.
- G. Carbone, M. Wicker, L. Laurenti, A. Patane, L. Bortolussi, and G. Sanguinetti. Robustness of bayesian neural networks to gradient-based attacks. *Advances in Neural Information Processing Systems*, 33:15602–15613, 2020.
- L. Cardelli, M. Kwiatkowska, L. Laurenti, N. Paoletti, A. Patane, and M. Wicker. Statistical guarantees for the robustness of bayesian neural networks. In *IJCAI*, 2019a.
- L. Cardelli, M. Kwiatkowska, L. Laurenti, and A. Patane. Robustness guarantees for bayesian inference with gaussian processes. In *Proceedings of the AAAI Conference on Artificial Intelligence*, volume 33, pages 7759–7768, 2019b.

- N. Carlini and D. Wagner. Adversarial examples are not easily detected: Bypassing ten detection methods. In *Proceedings of the 10th ACM Workshop on Artificial Intelligence and Security*, pages 3–14, 2017.
- P.-Y. Chen, H. Zhang, Y. Sharma, J. Yi, and C.-J. Hsieh. Zoo: Zeroth order optimization based black-box attacks to deep neural networks without training substitute models. In *Proceedings of the 10th ACM workshop on artificial intelligence and security*, pages 15–26, 2017.
- R. Christensen, W. Johnson, A. Branscum, and T. E. Hanson. *Bayesian ideas and data analysis: an introduction for scientists and statisticians*. CRC press, 2010.
- G. Cybenko. Approximation by superpositions of a sigmoidal function. *Mathematics of control, signals and systems*, 2(4):303–314, 1989.
- A. Fawzi, H. Fawzi, and O. Fawzi. Adversarial vulnerability for any classifier. In *Advances in Neural Information Processing Systems*, pages 1178–1187, 2018.
- R. Feinman, R. R. Curtin, S. Shintre, and A. B. Gardner. Detecting adversarial samples from artifacts. *arXiv preprint arXiv:1703.00410*, 2017.
- Y. Gal and L. Smith. Sufficient conditions for idealised models to have no adversarial examples: a theoretical and empirical study with bayesian neural networks. *arXiv preprint arXiv:1806.00667*, 2018.
- S. Goldt, M. Mézard, F. Krzakala, and L. Zdeborová. Modelling the influence of data structure on learning in neural networks. *arXiv preprint arXiv:1909.11500*, 2019.
- I. J. Goodfellow, J. Shlens, and C. Szegedy. Explaining and harnessing adversarial examples. *arXiv preprint arXiv:1412.6572*, 2014.
- K. Grosse, D. Pfaff, M. T. Smith, and M. Backes. The limitations of model uncertainty in adversarial settings. *arXiv preprint arXiv:1812.02606*, 2018.
- K. Grosse, M. T. Smith, and M. Backes. Killing four birds with one gaussian process: the relation between different test-time attacks. In *2020 25th International Conference on Pattern Recognition (ICPR)*, pages 4696–4703. IEEE, 2021.
- K. Hornik. Approximation capabilities of multilayer feedforward networks. *Neural networks*, 4(2):251–257, 1991.
- M. Khoury and D. Hadfield-Menell. On the geometry of adversarial examples. *CoRR*, abs/1811.00525, 2018. URL <http://arxiv.org/abs/1811.00525>.
- B. Lakshminarayanan, A. Pritzel, and C. Blundell. Simple and scalable predictive uncertainty estimation using deep ensembles, 2017.
- H. K. Lee. Consistency of posterior distributions for neural networks. *Neural Networks*, 13(6):629–642, 2000.

- J. M. Lee. Smooth manifolds. In *Introduction to smooth manifolds*, pages 1–31. Springer, 2013.
- Y. Li and Y. Gal. Dropout inference in bayesian neural networks with alpha-divergences. In *Proceedings of the 34th International Conference on Machine Learning-Volume 70*, pages 2052–2061. JMLR. org, 2017.
- X. Liu, Y. Li, C. Wu, and C.-J. Hsieh. Adv-bnn: Improved adversarial defense through robust bayesian neural network. *arXiv preprint arXiv:1810.01279*, 2018.
- A. Madry, A. Makelov, L. Schmidt, D. Tsipras, and A. Vladu. Towards deep learning models resistant to adversarial attacks, 2017.
- A. G. d. G. Matthews, M. Rowland, J. Hron, R. E. Turner, and Z. Ghahramani. Gaussian process behaviour in wide deep neural networks. *arXiv preprint arXiv:1804.11271*, 2018.
- R. Michelmore, M. Wicker, L. Laurenti, L. Cardelli, Y. Gal, and M. Kwiatkowska. Uncertainty quantification with statistical guarantees in end-to-end autonomous driving control. In *2020 IEEE International Conference on Robotics and Automation (ICRA)*, pages 7344–7350. IEEE, 2020.
- R. M. Neal. *Bayesian learning for neural networks*, volume 118. Springer Science & Business Media, 2012.
- R. M. Neal et al. Mcmc using hamiltonian dynamics. *Handbook of markov chain monte carlo*, 2(11):2, 2011.
- G. Ongie, R. Willett, D. Soudry, and N. Srebro. A function space view of bounded norm infinite width relu nets: The multivariate case. In *International Conference on Learning Representations*, 2020.
- Y. Pang, S. Cheng, J. Hu, and Y. Liu. Evaluating the robustness of bayesian neural networks against different types of attacks. *arXiv preprint arXiv:2106.09223*, 2021.
- A. Patane, A. Blaas, L. Laurenti, L. Cardelli, S. Roberts, and M. Kwiatkowska. Adversarial robustness guarantees for gaussian processes. *Journal of Machine Learning Research*, 23: 1–55, 2022.
- A. Rawat, M. Wistuba, and M.-I. Nicolae. Adversarial phenomenon in the eyes of bayesian deep learning. *arXiv preprint arXiv:1711.08244*, 2017.
- G. M. Rotskoff and E. Vanden-Eijnden. Neural networks as interacting particle systems: Asymptotic convexity of the loss landscape and universal scaling of the approximation error. *arXiv preprint arXiv:1805.00915*, 2018.
- A. Rozza, M. Manzo, and A. Petrosino. A novel graph-based fisher kernel method for semi-supervised learning. In *Proceedings of the 2014 22nd International Conference on Pattern Recognition, ICPR '14*, page 3786–3791, USA, 2014. IEEE Computer Society. ISBN 9781479952090. doi: 10.1109/ICPR.2014.650. URL <https://doi.org/10.1109/ICPR.2014.650>.

- L. Smith and Y. Gal. Understanding measures of uncertainty for adversarial example detection. *arXiv preprint arXiv:1803.08533*, 2018.
- D. Su, H. Zhang, H. Chen, J. Yi, P.-Y. Chen, and Y. Gao. Is robustness the cost of accuracy?—a comprehensive study on the robustness of 18 deep image classification models. In *Proceedings of the European Conference on Computer Vision (ECCV)*, pages 631–648, 2018.
- C. Szegedy, W. Zaremba, I. Sutskever, J. Bruna, D. Erhan, I. Goodfellow, and R. Fergus. Intriguing properties of neural networks. *arXiv preprint arXiv:1312.6199*, 2013.
- A. Uchendu, D. Campoy, C. Menart, and A. Hildenbrandt. Robustness of bayesian neural networks to white-box adversarial attacks. In *2021 IEEE Fourth International Conference on Artificial Intelligence and Knowledge Engineering (AIKE)*, pages 72–80. IEEE, 2021.
- A. W. v. d. Vaart. *Asymptotic Statistics*. Cambridge University Press, 2000. URL <https://EconPapers.repec.org/RePEc:cup:cbooks:9780521784504>.
- M. Wicker, L. Laurenti, A. Patane, and M. Kwiatkowska. Probabilistic safety for bayesian neural networks. In *Conference on Uncertainty in Artificial Intelligence*, pages 1198–1207. PMLR, 2020.
- M. Wicker, L. Laurenti, A. Patane, Z. Chen, Z. Zhang, and M. Kwiatkowska. Bayesian inference with certifiable adversarial robustness. In *International Conference on Artificial Intelligence and Statistics*, pages 2431–2439. PMLR, 2021.
- C. K. Williams and C. E. Rasmussen. *Gaussian processes for machine learning*, volume 2. MIT press Cambridge, MA, 2006.
- H. Xiao, K. Rasul, and R. Vollgraf. Fashion-mnist: a novel image dataset for benchmarking machine learning algorithms. *arXiv preprint arXiv:1708.07747*, 2017.
- N. Ye and Z. Zhu. Bayesian adversarial learning. In *Proceedings of the 32nd International Conference on Neural Information Processing Systems*, pages 6892–6901. Curran Associates Inc., 2018.
- M. Yuan, M. Wicker, and L. Laurenti. Gradient-free adversarial attacks for bayesian neural networks. *arXiv preprint arXiv:2012.12640*, 2020.
- J. Zhang, Y. Hua, Z. Xue, T. Song, C. Zheng, R. Ma, and H. Guan. Robust bayesian neural networks by spectral expectation bound regularization. In *Proceedings of the IEEE/CVF Conference on Computer Vision and Pattern Recognition*, pages 3815–3824, 2021.

A. Further Results

In what follows we present additional empirical results: in Section A.1 we add an experimental justification for Remark 7, while in Section A.2 we examine the relationship between BNNs and Deep Ensemble architectures.

A.1 Multimodal posterior distributions

Figure 6 empirically confirms remark 7, by showing that the posterior distributions of the weights are multimodal, thus Bernstein von Mises theorem does not apply to BNNs.

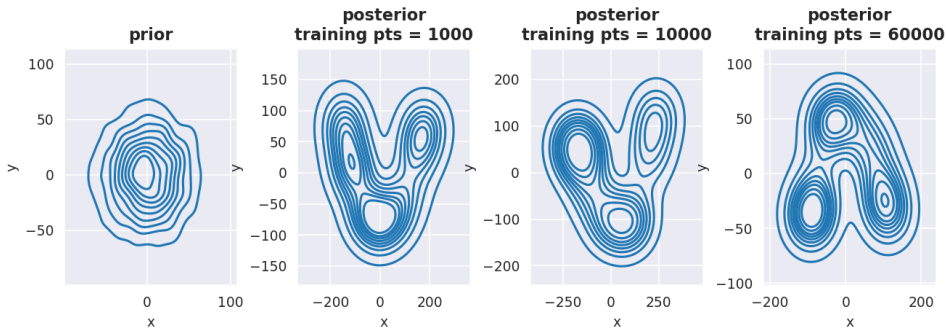


Figure 6: Prior (first column) and posterior (columns 1-3) distributions for models trained with an increasing number of training points. Models are trained on MNIST dataset with HMC. Samples are projected on the first two principal components (here x and y) using PCA.

A.2 Comparison with Deep Ensembles

Deep ensembles, as proposed by Lakshminarayanan et al. (2017), are an ensemble of neural networks trained from different randomly selected initial conditions, which are then averaged in order to make a prediction. In Table 2 we consider the same network used to perform the experiments in Section 6.2 (hyper-parameters are reported in Table 5) and run a comparison with both deterministic NNs and deep ensembles.

As expected, Bayesian NNs are more robust than deterministic ones. Moreover, we find that deep ensembles and deterministic NNs are comparable in terms of robustness, suggesting that simply averaging predictions for different weight initialization and mini-batching is not enough to achieve a robust model.

B. Training hyperparameters for BNNs

Tables 3, 6, 7 and 8 summarize the sets of hyperparameters used to tune our models. BNNs' architectures achieving the highest test accuracy are described in Table 4 for HMC training and 5 for VI training.

Model	Test accuracy	FGSM accuracy	PGD accuracy
Deterministic NN	97.69	21.19	1.45
Ensemble NN	99.4	20.6	0.3
Bayesian NN	96.1	90.0	89.8

Table 2: FGSM and PGD attacks on the network employed in Section 6.2. We compare a deterministic NN, a deep ensemble NN (of size 100), and a BNN (trained with VI). Attacks are performed on 1k test points from the MNIST dataset. We observe that VI trained network achieve better robustness against PGD and FGSM.

Half moons grid search	
Posterior samples	{250}
HMC warmup samples	{100, 200, 500}
Training inputs	{5000, 10000, 15000}
Hidden size	{32, 128, 256, 512}
Nonlinear activation	Leaky ReLU
Architecture	2 fully connected layers

Table 3: Hyperparameters for training BNNs in Figure 1

Training hyperparameters for HMC		
Dataset	MNIST	Fashion MNIST
Training inputs	60k	60k
Hidden size	1024	1024
Nonlinear activation	ReLU	ReLU
Architecture	Fully Connected	Fully Connected
Posterior Samples	500	500
Numerical Integrator Step size	0.002	0.001
Number of steps for Numerical Integrator	10	10

Table 4: Hyperparameters for training BNNs using HMC in Figures 2 and 3.

Training hyperparameters for VI

Dataset	MNIST	Fashion MNIST
Training inputs	60k	60k
Hidden size	512	1024
Nonlinear activation	Leaky ReLU	Leaky ReLU
Architecture	Convolutional	Convolutional
Training epochs	5	10
Learning rate	0.01	0.001

Table 5: Hyperparameters for training BNNs using VI in Figures 2 and 3.

HMC MNIST/Fashion MNIST grid search

Posterior samples	{250, 500, 750*}
Numerical Integrator Step size	{0.01, 0.005*, 0.001, 0.0001}
Numerical Integrator Steps	{10*, 15, 20}
Hidden size	{128, 256, 512*}
Nonlinear activation	{relu*, tanh, sigmoid}
Architecture	{1*,2,3} fully connected layers

Table 6: Hyperparameters for training BNNs with HMC in Figure 4. * indicates the parameters used in Table 1 of the main text.

SGD MNIST/Fashion MNIST grid search

Learning Rate	{0.001*}
Minibatch Size	{128, 256*, 512, 1024}
Hidden size	{64, 128, 256, 512, 1024*}
Nonlinear activation	{relu*, tanh, sigmoid}
Architecture	{1*,2,3} fully connected layers
Training epochs	{3,5*,7,9,12,15} epochs

Table 7: Hyperparameters for training BNNs with SGD in Figure 4. * indicates the parameters used in Table 1 of the main text.

SGD MNIST/Fashion MNIST grid search

Learning Rate	{0.001, 0.005, 0.01, 0.05}
Hidden size	{64, 128, 256, 512}
Nonlinear activation	{relu, tanh, sigmoid}
Architecture	{2, 3, 4, 5} fully connected layers
Training epochs	{5, 10, 15, 20, 25} epochs

Table 8: Hyperparameters for training BNNs with SGD in Figure 4.